

Overcoming Data Sparsity to Enable Deep Learning for Radiographic Non-Destructive Testing

Jacqueline Alvarez¹, Keith Henderson², Maurice Aufderheide², Brian Gallagher²,
Roummel F. Marcia¹, and Ming Jiang²

¹University of California, Merced, 5200 Lake Rd, Merced, CA 95343

²Lawrence Livermore National Laboratory, 7000 East Ave, Livermore, CA 94550

ABSTRACT

Radiography is an imaging technique used in various applications, such as medical diagnosis and airport security. We present a deep learning approach for extracting information from radiographic image data. We perform various prediction tasks using our approach, including material classification and regression on the dimensions of a given object that is being radiographed. Our framework is designed to fine-tune a pre-trained convolutional neural network using different datasets simulated by HADES, which is a radiographic simulation code. Moreover, we apply this framework to different types of radiographs including x-ray and neutron imaging.

Keywords: radiography, non-destructive testing, deep learning, classification, regression

INTRODUCTION

Radiography is widely used across various fields, including medical diagnosis, airport security, and non-destructive testing (NDT) [1, 2]. Industries such as aerospace, nuclear, and defense have high demands for quality assurance, thus, NDT plays a vital role in product inspection. Radiography offers benefits such as providing a permanent reference of an object's internal structure and being cost-effective. Computed Tomography (CT) is another valuable technique, providing three-dimensional data, albeit being more time-consuming and costly than 2D radiography [3]. Regardless of the method chosen, image processing is a requisite. The introduction of convolutional neural networks has revolutionized image processing; however, it requires substantial labeled data. Hence, we use high fidelity radiographic simulations to generate high-quality data and reduce the need for domain-dependent training.

METHODOLOGY

Radiographic Simulation: Deep learning requires a training set as large as possible. For radiographic applications, such a training set would be composed of “ground truth” objects and the radiographic images which would result from their being placed in a radiographic imaging system. It would be best to place them in such an imaging system and collect images which could then be paired with “ground truth”. Such an approach is not possible for several reasons. First, most of the objects are notional and the cost of building thousands of objects would be prohibitive. Second, existing radiographic imaging systems are time-intensive and expensive to use for collecting many images. Third, some of the radiographic systems themselves are notional and do not yet exist.

Because of these difficulties, it is necessary to use some form of radiographic simulation to generate the ensemble of training radiographs. There are many options for simulating radiography, but two main approaches are popular: monte-carlo simulation, and ray-trace simulation. In the monte-carlo approach, x-ray or gamma test particles are generated in a source (or the photon generation process is also modeled) and propagated toward the detector, allowing all manners of absorption, scattering and secondary photon generation to occur. MCNP [4] and Geant4 [5] are examples of monte-carlo codes which have been used for such simulation. Monte-carlo simulators can increase the physics accuracy of radiographic simulation but generally require a high level of expertise in radiation transport physics and are prohibitively expensive in terms of CPU time in order to collect reliable statistics for the desired radiographic images. At present, such a computationally expensive approach is unattractive for training sets. Another approach to generating simulated radiographs is to use ray-tracing techniques to cast rays between the

source and detector pixels and to compute the attenuation of the radiographic source by any objects between the source and detector. This approach enables quick generation of simulated radiographs, but they can lack physics verisimilitude, depending on what is included in the simulation. Examples of ray-tracing radiographic simulation codes are CIVA [6], XRSIM [7], XRaySim [8], and HADES [9].

In this work we have used the HADES radiographic simulation code because it is relatively fast, while including a good deal of radiographic physics. Also, HADES can ray trace through volumetric and surface meshes, as well as objects defined using solid constructive geometry through its link to BRL-CAD [10], an open-source CAD program. HADES has flexibility in simulating x-ray and gamma ray radiography (monochromatic or spectral) as well as neutron radiography (monochromatic or spectral). It also has the ability to include the effects of blur and noise properties of some imaging detectors, such as film, image plates and scintillators optically coupled to CCD cameras.

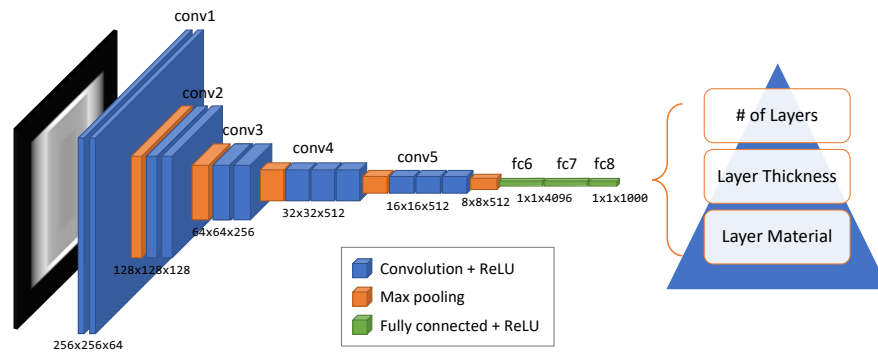


Figure 1: VGG network architecture for radiographic images.

Deep Learning: In this work, we utilize a pre-trained VGG neural network [11]. VGG is trained on ImageNet [12], which is a dataset with over a million images and 1000 object classes meaning that the network is likely to capture some basic features. We modify the network for each given task. This includes changing the number of input channels, since our images are single channel and VGG assumes 3-channel images. In addition, we adjust the output layer to be consistent with our dataset(s) since VGG is expecting 1000 outputs from ImageNet. For training, we utilize a variation of stochastic gradient descent method called AdamW with a learning rate of 10^{-5} . For the classification tasks, we use cross entropy as our loss function. For the regression models, we use MSE (mean squared error) for the loss. Figure 1 shows an example network for 256×256 images.



Figure 2: Example images comparing x-ray (left) and neutron (right) radiographs for the battery dataset.

EXPERIMENTS

We are interested in evaluating the performance of the VGG network for predicting the geometry and material for a given radiograph. For this evaluation, we created a battery dataset that consists of individual models of concentric cylinders composed of different materials. These are not intended to represent functional batteries, but rather objects that have similar geometries to batteries. For each layer of a battery, the material is selected from the following: gel, graphite, zinc, aluminum, beryllium, iron, lead, uranium, steel, and PMMA (acrylic). All simulated radiographs of batteries are 300×300 pixels (see Figure 2). There are two prediction tasks that we perform on the battery dataset. For the first task, we perform regression on the width of each layer of the battery. Since each battery varies in the number of layers it contains, predicting the width of each layer can be quite challenging. For the second task, we perform classification to identify the innermost layer material type.

Experiment 1 – Multi-Layer Regression: In previous experiments, we had a single model trained on a dataset where the batteries varied in the number of layers, making it difficult for the model to learn. We propose a two-step approach. The first step is to train a model to classify the number of layers of an object using the 2StepClassifier dataset. Since we are utilizing a pre-trained VGG model, we only need to train for 10 epochs. The second step is to train a regression model for each class (# of layers) using the 2StepRegressor datasets. This step in the process is more difficult, thus we needed to train each model for 200 epochs. For details on each dataset, see Table 1.

Table 1: List of datasets including image size, training/testing sizes, and number of classes/materials.

	Training	Testing	Task	# of layers	# of classes
2StepClassifier	28,000	7,000	classify	2–7	6
2StepRegressor	8,000	2,000	regression	per layer	-
5LayerBattery	16,000	4,000	classify	5	10

Experiment 2 – Material Classification: Next, we compare the performance of x-ray and neutron radiographs for classifying the innermost material of an object. X-ray sources are not able to penetrate dense materials as well as neutron sources, but neutrons are attenuated by some light materials (see Figure 2). Our goal is to compare the two imaging systems and see if we can leverage information from both sets of data. We train three models, where the first two models are trained on x-ray and neutron images, respectively. For the last model, we combine the x-ray and neutron images by stacking them as channels of an image. To simplify the evaluation, we use a subset of the batteries with only 5 layers (5LayerBattery) and train for 100 epochs.

Table 2: R^2 values for multi-layer regression on layer width.

Layer	0	1	2	3	4	5	6
Direct	0.58	0.38	0.14	0.19	0.29	0.28	0.18
2-Step	0.99	0.89	0.98	0.98	0.95	0.93	0.94

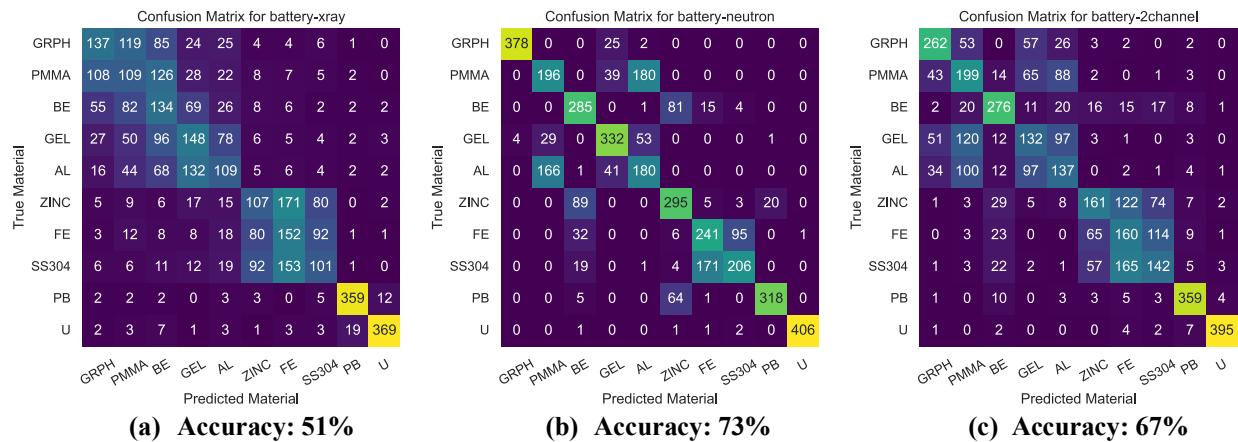


Figure 3: Confusion matrices for battery prediction results.

RESULTS

Experiment 1 – Multi-Layer Regression: Table 2 compares the performance of the simple multi-layer regression model with the two-step model. The simple model, which consists of a single regression model trained on all instances, performs best on Layer 0, the outermost layer, which is present in all instances. The performance degrades when predicting widths of more inner layers, because an increasing number of instances have zero width layers in those positions. The two-step model shows significant improvement in performance. This model outperforms the simple model on Layer 0, with the R^2 improving from 0.583 to 0.993. The degradation in performance on the inner layers is much less severe, with the worst case R^2 around 0.93 for the innermost layer of 6- and 7-layer batteries.

Experiment 2 – Material Classification: Figure 3 shows the accuracy of our models in predicting the innermost layer material for the 5LayerBattery. The model trained on neutron images outperforms the model trained on x-ray images. The model trained on two-channel inputs, stacking the x-ray and neutron images, did not outperform the neutron-only model. The objects in these datasets often have very dense outer shells, and the x-ray source cannot penetrate them. The x-ray model performs well predicting the densest materials (lead and uranium), but it performs poorly when trying to distinguish lighter materials, as they are often surrounded by dense layers. The neutron model does not suffer from this degradation, although it does confuse some of the lighter materials.

CONCLUSION

In this study, we demonstrate that leveraging high-fidelity physics simulations and pre-trained neural networks are effective in enabling deep learning models to reason about object composition and geometry. We evaluate our approach using both x-ray and neutron sources on simulated batteries. First, we propose a two-step approach for a multi-layer regression task, which improves the R^2 value of previous results by 70%. Next, we study the performance of x-ray and neutron imaging for material classification and note that neutron imaging improves the classification accuracy by 20%. We also implement a combined 2-channel approach, but this approach seems to be averaging the two results. Future work includes evaluating performance using additional datasets, studying the effects of noise in the data, and performing similar experiments with different x-ray sources.

ACKNOWLEDGEMENTS

This work was performed under the auspices of the U.S. Department of Energy by Lawrence Livermore National Laboratory under Contract DE-AC52-07NA27344, with funding provided by Kevin Mueller and Yuri Podpaly from the Defense Threat Reduction Agency. (LLNL-CONF-853736)

REFERENCES

- [1] Lopez, A., *et al.*, 2018. “Non-destructive testing application of radiography and ultrasound for wire and arc additive manufacturing,” *Additive Manufacturing*, vol. 21, pp. 298–306.
- [2] Wang, S. and Summers, R.M., 2012. “Machine learning and radiology,” *Medical Image Analysis*, vol. 16(5), pp. 933–951.
- [3] Hanke, R., Fuchs, T., and Uhlmann, N., 2008. “X-ray based methods for non-destructive testing and material characterization,” *Nuclear Instruments and Methods in Physics Research Section A: Accelerators, Spectrometers, Detectors and Associated Equipment*, vol. 591(1), pp. 14–18.
- [4] Briesmeister, J.F., *et al.*, 2000. “MCNP: a general monte carlo n-particle transport code,” *Los Alamos National Laboratory*, Version 4C, LA-13709-M.
- [5] Agostinelli, S., *et al.*, 2003. “Geant4—a simulation toolkit,” *Nuclear Instruments and Methods in Physics Research Section A: Accelerators, Spectrometers, Detectors and Associated Equipment*, vol. 506(3), pp. 250–303.
- [6] CIVA. <https://www.extende.com/civa-in-a-few-words>.
- [7] Nondestructive evaluation techniques: Radiography. <https://www.nde-ed.org/NDETechniques/Radiography/AdvancedTechniques/xrsim.xhtml>.
- [8] XRaySim. <https://xraysim.sourceforge.net/index.htm>.
- [9] Aufderheide, M.B., *et al.*, 2004. “HADES, a code for simulating a variety of radiographic techniques,” *IEEE Symposium Conference Record Nuclear Science*, vol. 4, pp. 2579–2583.
- [10] BRL-CAD open source project. <http://brlcad.org/>.
- [11] Simonyan, K. and Zisserman, A., 2015. “Very deep convolutional networks for large-scale image recognition,” *International Conference on Learning Representations*, pp. 1–14.
- [12] Deng, J., Dong, W., Socher, R., Li, L.J., Li, K. and Fei-Fei, L., 2009. “ImageNet: A large-scale hierarchical image database,” *IEEE Conference on Computer Vision and Pattern Recognition*, pp. 248–255.